NANO LETTERS

2008
Vol. 8, No. 4
1066-1070

DNA Sensing by Silicon Nanowire: Charge Layer Distance Dependence

Guo-Jun Zhang,* Gang Zhang, Jay Huiyi Chua, Ru-Ern Chee, Ee Hua Wong, Ajay Agarwal, Kavitha D. Buddharaju, Navab Singh, Zhiqiang Gao,† and N. Balasubramanian

Institute of Microelectronics, Agency for Science, Technology and Research, 11 Science Park Road, Singapore 117685

Received November 16, 2007; Revised Manuscript Received January 21, 2008

ABSTRACT

To provide a comprehensive understanding of the field effect in silicon nanowire (SiNW) sensors, we take a systematic approach to fine tune the distance of a charge layer by controlling the hybridization sites of DNA to the SiNW preimmobilized with peptide nucleic acid (PNA) capture probes. Six target DNAs of the same length, but differentiated successively by three bases in the complementary segment, are hybridized to the PNA. Fluorescent images show that the hybridization occurs exclusively on the SiNW surface between the target DNAs and the PNA. However, the field-effect response of the SiNW sensor decreases as the DNA (charge layer) moves away from the SiNW surface. Theoretical analysis shows that the field effect of the SiNW sensor relies primarily on the location of the charge layer. A maximum of 102% change in resistance is estimated based on the shortest distance of the DNA charge layer (4.7 Å) to the SiNW surface.

Silicon nanowires (SiNWs) have widely been developed over the past few years as ultrasensitive biosensors and chemical sensors. Successful applications of SiNW sensors have been demonstrated for ions,[1,2] DNA,[3–7] proteins,[1,8,11] virus,[9] and cells,[10,11] Thanks to a large surface-to-volume ratio, tunable electrical properties, and biocompatibility, the SiNWs would prove to be ultrasensitive, label-free electrical sensors. For SiNW DNA sensors in particular, the sensing mechanism by SiNWs can be understood in terms of the change in charge density which induces a change in electric field at the SiNW surface after hybridization. As a consequence of the field-effect-based sensing mechanism, the distance of the DNA (charge layer) to the SiNW surface plays a key role in the detection sensitivity. The first example of SiNW pH sensing, using a (3-aminopropyl)triethoxysilane coated p-type SiNW, exhibited approximately 140% conductance change from pH 2 to 9.[1] On the other hand, only 46% conductance change was observed on another SiNW sensor where a rather long spacer was used to link up PNA capture probes and the SiNW.[4] Even much smaller changes were observed in the case of protein sensing, possibly due to the bulky size of proteins increasing the effective distance of the charges from the SiNW surface.[1]

For the SiNW biosensors, the field effect is affected by many factors such as Debye screening,[12] SiNW size,[13] surface chemistry,[7] and so on. However, to date there are not yet sufficient experimental data and theoretical simulation for these field-effect-based devices that will be able to further make clear the effect on detection sensitivity.

Scheme 1. Schematic Representation of Variation of the Field Effect of the SiNW Sensor Caused by Varying Hybridization Sites of Target DNA to PNA

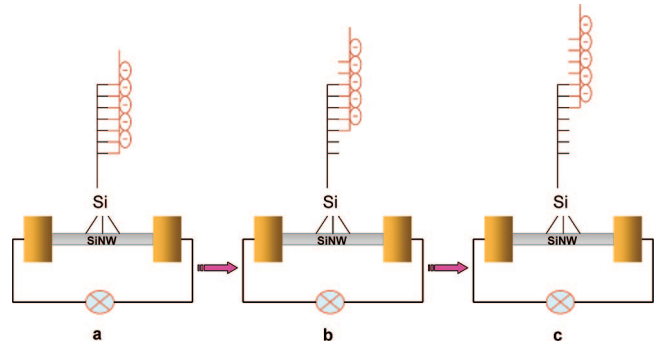

To study the influence of the distance of the charge layer to the SiNW surface on the detection sensitivity and the limitations of field-effect-based SiNW sensing devices, herein we design an approach to vary the distance of the charge layer by varying the hybridization sites of DNAs to the peptide nucleic acid (PNA) capture probes while maintaining the total number of charges unchanged. Our results show that the detection sensitivity is determined by the distance of the hybridized target DNA layer to the SiNW surface with good correlation to our theoretical analysis. Nonetheless, both experimental data and theoretical analysis suggest that the relatively low analytical signal intensity (in terms of signal/

* Corresponding author: tel, +65-6770-5390; fax, +65-6774-5754; e-mail, zhanggj@ime.a-star.edu.sg.

† Current address: Institute of Bioengineering and Nanotechnology, 31 Biopolis Way, The Nanos, #04-01, Singapore 138669.

10.1021/nl072991l CCC: $40.75
Published on Web 03/01/2008

Table 1. Sequences of PNA Capture Probes and Target DNAs and Calculated Distances from the SiNW Surface of the DNAs upon Hybridization with PNA

		sequences	near side distances of DNAs from the SiNW surface (Å)
	PNA	N-NH_2-AAC CAC ACA ACC TAC TAC CTC A-C	
1	fully complementary DNA	5′-TGA GGT AGT AGG TTG TGT GGT T-3′	26.4
2	19-nt complementary DNA	5′-AAA TGA GGT AGT AGG TTG TGT G-3′	36.6
3	16-nt complementary DNA	5′-AAA AAA TGA GGT AGT AGG TTG T-3′	46.8
4	13-nt complementary DNA	5′-AAA AAA AAA TGA GGT AGT AGG T-3′	57.0
5	10-nt complementary DNA	5′-AAA AAA AAA AAA TGA GGT AGT A-3′	67.2
6	7-nt complementary DNA	5′-AAA AAA AAA AAA AAA TGA GGT A-3′	77.4
7	noncomplementary DNA	5′-ATG CAT GCA TGC ATG CAT GCA A-3′	

unit concentration) is one of the grand challenges that need to be addressed in the development of SiNW sensors.

A schematic illustration of the distance change induced by the controlled hybridization of PNA−DNA is given in Scheme 1. The PNA capture probes with amine groups at their N ends are covalently immobilized on the SiNW surface by means of photochemical hydrosilation. The reason for using PNA instead of DNA as capture probes is to produce ultralow background electric charges as PNA is neutral and to increase the hybridization efficiency. The neutral character of the PNA backbone alleviates the formation of a dense charge layer and allows hybridization to take place at low ionic strength, minimizes the build-up of a strong electrical field at the SiNW surface, and hence reduces the background, producing a high signal/noise ratio. Moreover, the PNA capture probes have a greater affinity and stability than their DNA counterparts at low ionic strength where a low background signal is observed, again due to their neutral character which eliminates electrostatic repulsion between the two hybridized strands.[14] Six 22-nucleotide (nt) target DNAs, namely, a fully complementary, a 19-nt complementary, a 16-nt complementary, a 13-nt complementary, a 10-nt complementary, and a 7-nt cDNA, are used in this study. A 22-nt noncDNA was used as control. The sequences of the PNA capture probes and the target DNAs are listed in Table 1 along with the calculated near-side distance of DNA from the SiNW surface. All DNAs have exactly the same length as PNA (22-nt). Quantitative fluorescence measurement of hybridization of the six different target DNAs labeled with Cy 3 to the immobilized PNA and the corresponding melting temperatures of each PNA/DNA duplex are described (Figures 1 and 2 in Supporting Information and Table 1 in Supporting Information, respectively). The results demonstrate that these

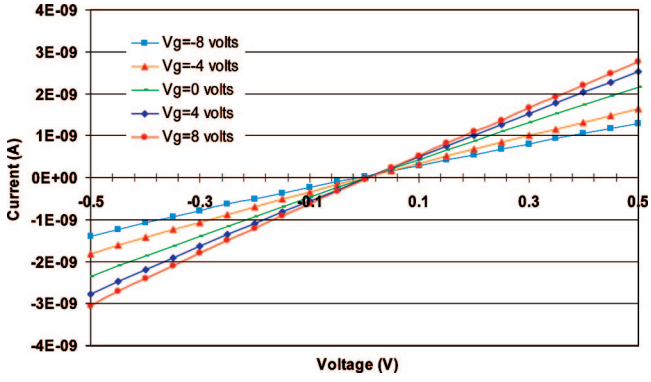

Figure 1. Typical $I-V$ curves at various back-gate biasing.

Table 2. Measured Contact Angles for the Si(100) Surface at Various Functionalized Stages

surface	contact angle, θ (deg)
native oxide surface	10.1
hydrogen-terminated surface	82.1
t-BOC protected amine surface	78.3
amine-terminated surface	51.6

DNAs are capable of fully hybridizing themselves to the PNA capture probes, thereby resulting in the formation of charge layers with the same number of charges, but with different distances to the SiNW surface. Consequently, the field effect of the SiNWs is different in each case, leading to the distinguishable variation in the detection sensitivity.

The device fabrication is described in Supporting Information and will not be depicted here. The devices were fabricated in polysilicon layers deposited on the thermally grown oxide on p-type test wafers. To verify the quality of the SiNW arrays, a current–voltage ($I-V$) curve with the back-gate response was obtained electrically prior to the functionalization of the SiNWs. Figure 1 illustrates typical $I-V$ curves at various back-gate biasing. Plots show an ohmic behavior as expected of a typical resistor. The resistance of these N-type nanowires increases as the back-gate bias changes from 0 to –8 V (due to carrier depletion) while their resistance decreases, as the charge accumulates by the application of positive back-gate potential. The device was operated at 0.2 V for all sensing experiments.

As the dimension of the SiNWs used is a few tens of nanometers, it is challenging to characterize surface functionalization on the SiNWs using XPS. Hence, Si(100) bulk wafer surfaces were utilized to undergo the same functionalization process as described elsewhere and surface analysis.[15,16] Contact angle measurement which provides a measurement of surface hydrophobicity was used to follow the functionalization procedures of various surfaces. Table 2 shows a small contact angle of 10.1° for the native oxide covered Si surface and a large contact angle of 82.1° for the freshly prepared hydrogen-terminated Si surface, reflecting the hydrophobic nature of the Si surface after removal of native oxide layer and termination with hydrogen. Furthermore, after treatment of the surface with t-BOC protected amine using photochemistry, the contact angle measured is 78.3°, meaning the surface is still predominantly hydrophobic. The contact angle decreases to 51.6° after further treatment of the surface with TFA and ammonium solution, resulting from the decrease in hydrophobicity because the surface is terminated with amine groups.

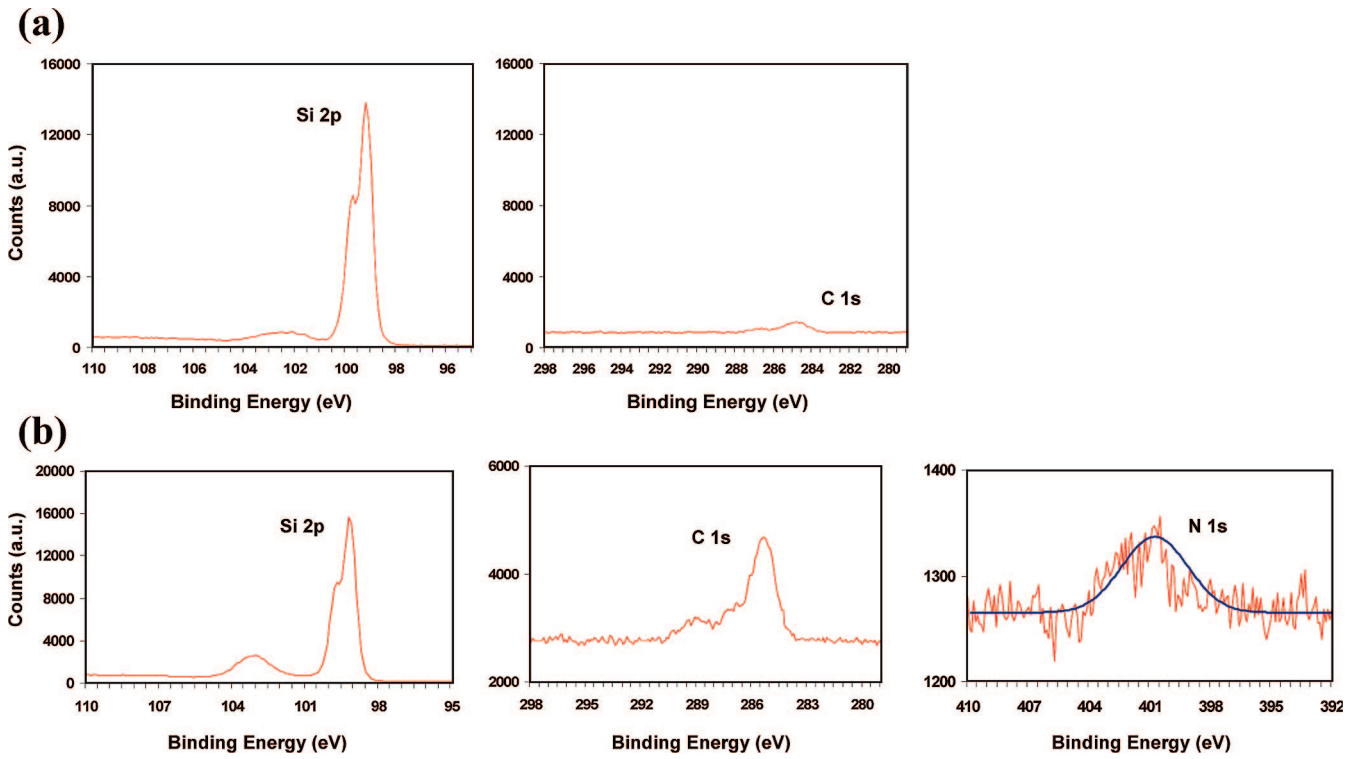

Figure 2. X-ray photoelectron spectra of the hydrogen-terminated and the amine-functionalized Si(100) surface. (a) The hydrogen-terminated surface only shows Si(2p) and very weak C(1s) peaks. (b) The amine-functionalized surface shows a N(1s) peak in addition to Si(2p) and C(1s) peaks.

To understand more details on surface functionalization, X-ray photoelectron spectroscopy (XPS) was performed to characterize the nature of surface-bound species, especially the amine-modified surface in this experiment. Figure 2 shows XPS data for the nitrogen (1s), silicon (1s), and carbon (1s) core levels on the Si(100) surface after surface functionalization. One control experiment is presented, in which the surface was hydrogen-terminated. The hydrogen-terminated surface shows a bulk Si peak (102.1 eV) but a small C signal likely because of physically adsorbed hydrocarbons, which is consistent with the results obtained previously (Figure 2a).[17] As can be seen in Figure 2b, after the surface was treated with t-BOC protected amine by photochemistry and terminated with amine groups after deprotection, the N(1s) spectrum shows a strong peak with a binding energy of 400.5 eV, corresponding to free amine on the surface. In addition, the C(1s) spectrum similarly shows a peak with a binding energy of 285.4 eV, contributed by the carbon chain of the decene. The Si(2p) spectrum (103.1 and 99.2 eV) was also observed from the surface in this stage and showed no detectable levels of oxidation. These results demonstrate the amine-functionalized silicon surface was constructed via photochemistry as illustrated in Scheme 1 in the Supporting Information.

To demonstrate the selective surface chemistry and the sequence specificity, the fully complementary, the seven-base complementary, and the control labeled with Cy 3 at their 5′ ends were applied to the SiNW sensors. The SiNWs were then characterized under epi-fluorescence microscopy (Figure 3). Strong fluorescent signals on the SiNWs were observed, and the bright arrays of SiNWs were clearly visible when the fully complementary target DNA was hybridized to the PNA (Figure 3a). The fluorescent SiNW arrays are regularly shaped with high uniformity, corresponding to those observed by SEM image.[6] Remarkably, the 7-base complementary target DNA exhibited the same brightness, as shown in Figure 3b. On the contrary, almost no fluorescent signals could be seen when the noncomplementary target DNA was employed (Figure 3c). These results reveal that the complementary target DNAs were completely hybridized to the immobilized PNA as expected and confirm the specificity of binding between the target DNAs and the PNA. Moreover, fluorescent signals were observed only at the SiNW surface, implying that the photochemical hydrosilation used for immobilizing the PNA capture probes are highly selective to the SiNWs, against SiO_2, offering an excellent opportunity for theoretical simulation since any hybridization taking place on the substrate (SiO_2) in the vicinity of the SiNW will complicate the theoretical model.

Debye length is obviously one of the significant factors, which affects the detection sensitivity. It in principle depends on the ionic strength of electrolyte solution. To detect the hybridized DNAs which are located at more than a few nanometers from the SiNWs and differentiate the influence of the distance in the charged molecules, 0.01 × SSC (0.15 mM sodium citrate, 1.5 mM NaCl, pH 7.4) buffer solution is employed because it has a Debye length ~10 nm, which allows the hybridization distance effect detectable.

The resistance of the n-type SiNW sensor increases with the accumulation of negative charges upon hybridization. Figure 4 shows the resistance changes caused by the hybridization of the target DNAs with the PNA at two

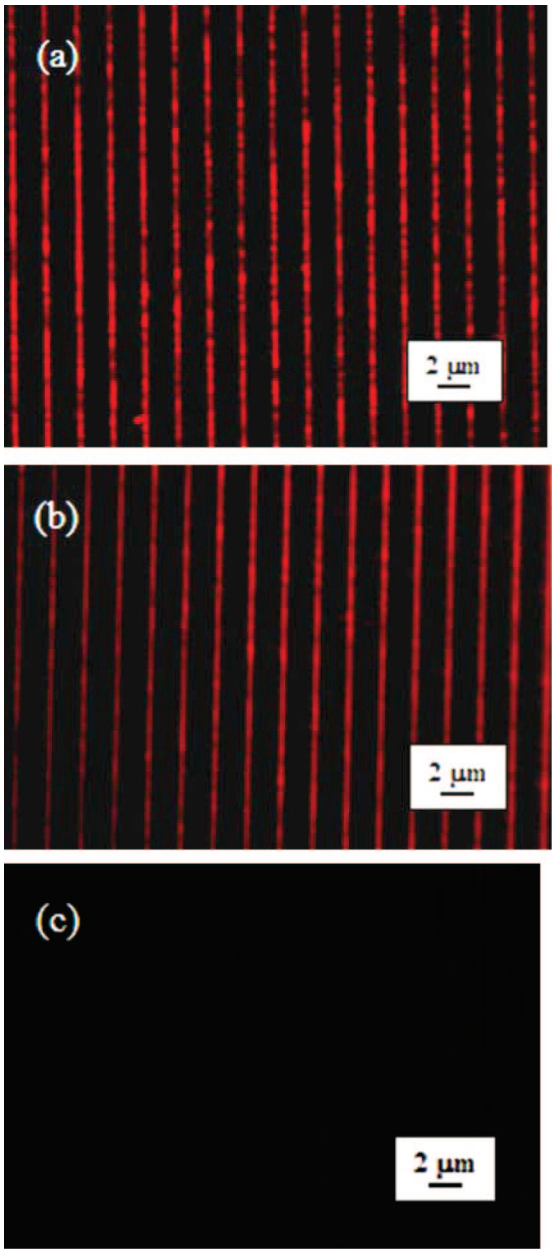

Figure 3. Fluorescent images of Cy 3-labeled DNAs hybridized to the PNA-functionalized SiNW: (a) Cy 3-labeled fully cDNA; (b) Cy 3-labeled seven-base cDNA; (c) noncomplementray DNA.

different concentrations. The control experiment yielded a barely visible resistance change upon hybridization with 1 nM of the noncomplementary target DNA and no measurable response at 1 pM. The small resistance change observed at 1 nM suggests that there is probably some nonspecific binding of the noncomplementary DNA on the SiNW surface. When the PNA-functionalized SiNWs were treated with 1 nM of the fully complementary target DNA, a resistance change (∼51%) was observed. In a similar way, resistance changes due to the PNA−DNA hybridization between the other target DNAs and the PNA were recorded. Direct comparison of these results highlights that the resistance change is closely associated with the hybridization sites of the cDNAs to PNA. Figure 4 reveals that the

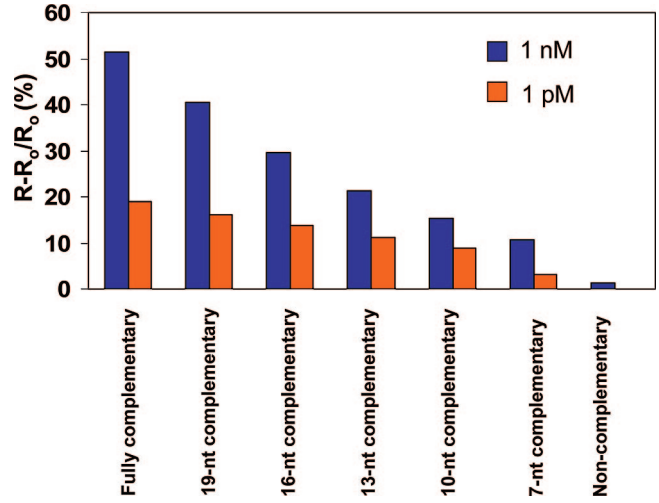

Figure 4. Distinguishable resistance change of the SiNW caused by varying hybridization sites at two different concentrations of the target DNAs.

resistance change decreases with the hybridization sites moving away from the SiNW surface. For example, only ∼11% resistance change was obtained for the seven-base complementary target DNA under identical conditions. These data qualitatively demonstrate that the SiNW sensor highly relies on the location of the charge layer to which the target DNA lies and the corresponding detection sensitivity is greatly dependent on the distance of the charge layer to the SiNW surface, true to a field-effect-based sensor.

Further confirmation was demonstrated by the hybridization of the six target DNAs with the PNA at a much lower concentration of 1 pM. At 1 pM, the fully complementary target DNA generated ∼19% resistance change, whereas only 3.5% change was obtained in the case of the 7-base complementary target DNA. Nonetheless, the general trend of the resistance change at 1 pM is consistent with that at 1 nM.

DNA orientation near the surface is very important and it relates to the charge layer distance dependence in this work. However, it is still difficult, or even impossible in many cases, to obtain an atomistic picture of DNA near a surface. PNA is an achiral and uncharged DNA mimic, which leads to an ordered layer on a surface because PNA avoids the strong electrostatic molecule−molecule and molecule−surface interactions and the PNA molecule is more rigid than DNA. Briones et al.[18] studied a gold surface formed with ordered self-assembled monolayers of single-stranded PNA. With an appropriate spacer, the PNA molecules stand vertically on a gold surface regardless of their remarkable length (7 nm). Moreover, an all-atom molecular dynamics simulation of DNA on a silica surface[19] also showed that after the system reached a stationary state, the DNA established an upright position on the surface and the polar angle between the DNA helical axis and the surface normal fluctuated around 10°. On the basis of the theoretical simulation and the experimental conclusion, upright orientation of the designated PNA on the SiNW surface is preferable because the spacer between PNA and the surface is carbon chains 15 atoms in

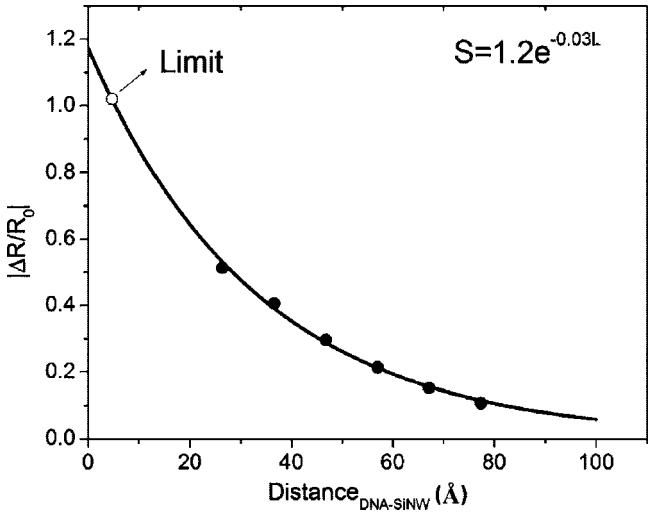

Figure 5. Plots of the experimental $|\Delta R/R_0|$ vs calculated distance of DNA strands to the SiNW *L*. The filled circles are the experimental data and the solid line is the least-squares fit to the data. The open circle is the extrapolated limit.

length. Here we made an assumption that the hybridized DNAs are perpendicular to the SiNW surface.

Using the spacer length between PNA and the Si surface and the separation between DNA base pairs (3.4 Å),[20] we calculated the distance of DNA strands to the SiNW as shown in Table 1 (defined as the distance between the lowest DNA base and the SiNW surface). With the experimental resistance data and the distance of DNA strands to the SiNW, *L*, we plotted the experimental $|\Delta R/R_0|$ vs *L* curve in Figure 5 ($\Delta R = R - R_0$, $S = |\Delta R/R_0|$). For the fully cDNA, the calculated distance is 26.4 Å, and for the seven-base cDNA, it is 77.4 Å. As the distance of DNA strands to the SiNW increases from the fully complementary to the seven-base cDNA (Table 1), the effective electrostatic potential and hence the magnitude of resistance change decreases, as experimentally aforementioned. It is observed that the relative change of resistance decreases with increase in *L* as $S = 1.2e^{-0.03L}$. This exponential relation is consistent with the result that, in a small effective electrostatic potential range, the relative resistance change depends on electrostatic potential linearly[21] and the electrostatic potential created by charge layer depends on distance exponentially in solution.[22] The good exponential dependence shows that our SiNW sensors with the effective electrostatic potential created by the target DNAs work nearly as an ideal transistor. Theoretically, the shortest distance of the DNA strands to the SiNW surface is 4.7 Å, corresponding to a resistance change of 102%.

In summary, we have demonstrated a systematic approach to clarifying that the detection sensitivity of the field-effect-based SiNW sensors is significantly dependent on the distance of the DNA charge layer to the SiNW surface. The field effect gets much weaker if the charge layer is farther apart from the SiNW sensor surface. This effect has also been demonstrated by theoretical analysis for the calculated distance of DNA strands to the SiNW surface and further charge layer dependence. Our results demonstrate the significance of charge layer distance to ensure SiNW biosensing sensitivity. The work enables us to understand the response of the SiNW biosensors to the location of charge layer.

Acknowledgment. The authors thank Dr. Julien Reboud for his assistance with contact angle measurements. We also acknowledge Zheng Zhang and Nelvi Sutanto at the Institute of Materials Research and Engineering in Singapore for their assistance with XPS spectra.

Note Added after ASAP Publication: This paper was published ASAP on March 1, 2008. An author affiliation was changed. The revised paper was reposted on March 7, 2008.

Supporting Information Available: Descriptions of experimental details, figures showing fluorescence images, comparisons of fluorescence intensity of hybridization, and real time detection of DNA, and table showing predicted T_m for PNA/DNA duplexes. This material is available free of charge via the Internet at http://pubs.acs.org.

References

(1) Cui, Y.; Wei, Q. Q.; Park, H. K.; Lieber, C. M. *Science* **2001**, *293*, 1289.
(2) Zhang, G.-J.; Agarwal, A.; Buddharaju, K. D.; Singh, N.; Gao, Z.-Q. *Appl. Phys. Lett.* **2007**, *90*, 233903.
(3) Hahm, J.-I.; Lieber, C. M. *Nano Lett.* **2004**, *4*, 51.
(4) Li, Z.; Chen, Y.; Li, X.; Kamins, T. I.; Nauka, K.; Williams, R. S. *Nano Lett.* **2004**, *4*, 245.
(5) Li, Z.; Rajendran, B.; Kamins, T. I.; Li, X.; Chen, Y.; Williams, R. S. *Appl. Phys. A: Mater. Sci. Process.* **2005**, *80*, 1257.
(6) Gao, Z.-Q.; Agarwal, A.; Trigg, A. D.; Singh, N.; Fang, C.; Tung, C.-H.; Fan, Y.; Buddharaju, K. D.; Kong, J.-M. *Anal. Chem.* **2007**, *79*, 3291.
(7) Bunimovich, Y. L.; Shin, Y. S.; Yeo, W.-S.; Amori, M.; Kwong, G.; Heath, J. R. *J. Am. Chem. Soc.* **2006**, *128*, 16323.
(8) Zheng, G.; Patolsky, F.; Cui, Y.; Wang, W. U.; Lieber, C. M. *Nat. Biotechnol.* **2005**, *23*, 1294.
(9) Patolsky, F.; Zheng, G.; Hayden, O.; Lakadamyali, M.; Zhuang, X.; Lieber, C. M. *Proc. Natl. Acad. Sci. U.S.A.* **2004**, *101*, 14017.
(10) Patolsky, F.; Timko, B. P.; Yu, G.; Fang, Y.; Greytak, A. B.; Zheng, G.; Lieber, C. M. *Science* **2006**, *313*, 1100.
(11) Stern, E.; Klemic, J. F.; Routenberg, D. A.; Wyremebak, P. N.; Turner-Evans, D. B.; Hamilton, A. D.; LaVan, D. A.; Fahmy, T. M.; Reed, M. A. *Nature* **2007**, *445*, 519.
(12) Stern, E.; Wagner, R.; Sigworth, F. J.; Breaker, R.; Fahmy, T. M.; Reed, M. A *Nano Lett.* **2007**, *7*, 3405.
(13) Elfström, N.; Juhasz, R.; Sychugov, I.; Engfeldt, T.; Karlström, A. E.; Linnros, J. *Nano Lett.* **2007**, *7*, 2608.
(14) Paulasova, P.; Pellestor, F *Ann. Genet.* **2004**, *47*, 349.
(15) Strother, T.; Hamers, R. J.; Smith, L. M. *Nucleic Acids Res.* **2000**, *28*, 3535.
(16) Streifer, J. A.; kim, H.; Nichols, B. M.; Hamers, R. J. *Nanotechnology* **2005**, *16*, 1868.
(17) Lin, Z.; Strother, T.; Cai, W.; Cao, X.; Smith, L. M.; Hamers, R. J. *Langmuir* **2002**, *18*, 788.
(18) Briones, C.; Mateo-Marti, E.; Gomez-Navarro, C.; Parro, V.; Roman, E.; Martin-Gago, J. A. *Phys. Rev. Lett.* **2004**, *93*, 208103.
(19) Wong, K-Y.; Pettitt, B. M. *Biopolymers* **2004**, *73*, 570.
(20) (a) Kuchitsu, K. *Structure of Free Polyatomic Molecules- Basic Data*; Springer: Berlin, 1998. (b) Berman, H. M.; Westbrook, J.; Feng, Z.; Gilliland, G.; Bhat, T. N.; Weissig, H.; Shindyalov, I. N.; Bourne, P. E. *Nucleic Acids Res.* **2000**, *28*, 235.
(21) Wang, J.; Polizzi, E; Lundstrom, M *J. Appl. Phys.* **2004**, *96*, 2192.
(22) Bruesch, P.; Christen, T. *J. Appl. Phys.* **2004**, *95*, 2846.

NL072991L